Analytical Solutions to Coupled HM Problems to Highlight the Nonlocal Nature of Aquifer Storage

Article *in* Water Resources Research · October 2017

DOI: 10.1002/2017WR020824

2 authors:

Silvia De Simone
Imperial College London
12 PUBLICATIONS **88** CITATIONS
SEE PROFILE

Jesús Carrera Ramírez
Spanish National Research Council
468 PUBLICATIONS **10,899** CITATIONS
SEE PROFILE

De Simone, S., Carrera, J. (2017). Analytical solutions to coupled HM problems to highlight the nonlocal nature of aquifer storage. *Water Resources Research*, 53(11), 9580-9599.

Analytical solutions to coupled HM problems to highlight the non-local nature of aquifer storage

Silvia De Simone [1,2,3] **and Jesús Carrera** [1,3]

[1]Institute of Environmental Assessment and Water Research (IDAEA), CSIC, c/ J. Girona 18, 08034 Barcelona, Spain

[2]Department of Civil and Environmental Engineering, Universitat Politécnica de Catalunya (UPC), c/ J. Girona 1-3, 08034 Barcelona, Spain

[3]Associated Unit: Hydrogeology Group (UPC-CSIC)

Key Points:

- Storage depends not only on aquifer compressibility, but also on its geometry and surrounding formations
- Analytical solutions to transient pressure acknowledging hydro-mechanical coupling
- Hydro-mechanical pressure response to injection/extraction is different respect to traditional solution

Corresponding author: Silvia De Simone, silviadesi@gmail.com

Abstract

Specific storage reflects the volumetric deformation capacity of permeable media. Classical groundwater hydrology equates elastic storage to medium compressibility (plus fluid compressibility times porosity). However, it is unclear if storage behavior can be represented by a single parameter. Hydraulic gradients act as body forces that push the medium in the direction of flow causing it to deform instantaneously everywhere, i.e., even in regions where pressure would not have changed according to conventional fluid flow. Therefore, actual deformation depends on the mechanical properties of the medium, but also on aquifer geometry and on surrounding strata, which act like constraints to displacements. Here we discuss the question and highlight the non-local nature of storage (i.e., the volume of water released at a point depends on the poroelastic response over the whole aquifer). Proper evaluation of transient pressure and water release from storage requires acknowledging the hydro-mechanical coupling, which generally involves the use of numerical methods. We propose analytical solutions to the HM problem of fluid injection (extraction) into finite aquifers with one-dimensional or cylindrical geometries. We find that pressure response is much faster (virtually instantaneous) and larger than expected from traditional purely hydraulic solutions when aquifer deformation is restrained, whereas the pressure response is reversed (i.e., pressure drop in response to injection) when the permeable medium is free to deform. These findings suggest that accounting for hydro-mechanical coupling may be required when hydraulic testing is performed in low permeability media, which is becoming increasingly demanded for energy-related applications.

1 Introduction

Specific storage (S_s) is defined as the volume of water released per unit volume of aquifer per unit drop in head [*Hantush*, 1961]. Despite its importance, the very concept of storage has been the subject of an extensive and animated discussion since *Meinzer* [1928] conceived that idea that “aquifers are compressible and elastic" [*Narasimhan*, 2006]. Therefore, *Jacob* [1940] expressed S_s the way it is used nowadays by assuming deformation to be primarily vertical, which is reasonable for the extensive aquifers that motivated his work, thus finally establishing the flow equation. A consequence of this equation is that heads will start responding to pumping after about $0.1t_c$, where $t_c = S_s r^2/(\kappa)$ is the characteristic response time, r is distance to the pumping well, κ is hydraulic conductivity. This time can be sizable when κ is small. Yet, virtually instantaneous response is

50 often recorded, especially in low permeability media (e.g., *Blocher et al.* [2008]). Worse,
51 head drops have been reported in response to injection (e.g., *Batchelor* [1983]; *Slack et*
52 *al.* [2013]). Instantaneous and reverse pressure response can be attributed to poroelastic
53 effects, because water injection (pumping) causes an increase (decrease) in fluid pressure
54 that acts as a load at the well and causes deformation (and variations in porosity) around
55 the well. These effects can be reproduced performing coupled hydro-mechanical mod-
56 els, which are rarely used by hydrogeologists (e.g., *Berg et al.* [2011]), possibly because
57 fluid pressure buildup in conventional aquifers is moderate. Yet, given, the increasing de-
58 mand for hydraulic testing in low permeability media (e.g., enhanced geothermal systems
59 or shale gas), it is clear that the validity of the traditional equation for flow through porous
60 media needs to be questioned and analyzed, which warrants revising the meaning of stor-
61 age.

62 Underlying this discussion is the need to distinguish between storage as a “behav-
63 ior" and storage as a “property" (Hsieh, 2017, personal communication). The term behav-
64 ior refers to the concept that a drop in head drives the release of water. The term prop-
65 erty refers to the measured quantity (or function of other measurable quantities) needed to
66 quantify this behavior. Actually, this study is largely motivated by a third related concept,
67 namely, the way in which this behavior is represented in fluid mass conservation equation.
68 For example, the storage “behavior" is usually represented by the term $S_s \partial h/\partial t$, where S_s
69 is the specific storage coefficient (i.e, “property") and h is head. The initial definition [*Ja-*
70 *cob*, 1940] of storage coefficient equated the behavior and the property by assuming that
71 the pumped aquifer deforms only in the vertical direction. In fact, the initial definition was
72 vertically integrated. Actually, transient flow is coupled to mechanical equilibrium because
73 fluctuations in head (pore pressure) cause changes in effective stresses [*Terzaghi*, 1923;
74 *Biot*, 1941] that drive three-dimensional deformations. Therefore, the problem has to be
75 formulated as a coupled hydro-mechanical (HM) one to properly represent these defor-
76 mations, which altogether eliminates the need for defining an explicit storage coefficient.
77 While the HM coupled nature of the problem is widely acknowledged, the assumption
78 of vertical deformation has remained common practice by hydrogeologists because solv-
79 ing HM problem is complex. Yet, the issue is not free of debate. Several authors have
80 argued that pumping causes non negligible horizontal displacements [*Poland and Davis*,
81 1969; *Gambolati*, 1974; *Bear and Corapcioglu*, 1981; *Helm*, 1994]. The topic is well ad-
82 dressed by *Burbey* [1999, 2001], who also illustrates the analytic derivation of uniaxial

and volumetric storage coefficients starting from elasticity theory and compares the effects of considering or not the horizontal displacements. In fact, *Hsieh and Cooley* [1995] show that horizontal displacements can be neglected when the under- and/or overlying layers are somewhat stiff.

Whether or not horizontal strains are acknowledged, it is clear that the storage behavior depends on the factors (dimension, flow geometry, boundary conditions, etc.) that control volumetric deformation. In fact, poroelasticity allows one to distinguish between two “extreme" (plus other “intermediate") specific storage concepts [*Wang*, 2000]: (1) unconstrained specific storage, when the total stress remains unaffected by pressure changes, and (2) constrained specific storage, when it is strain that remains unaffected. By itself, the distinction suggests that storage at a point depends on the HM response of the whole aquifer system, which means that storage behavior is non-local.

The implication is that it is not possible to characterize the storage behavior using a constant in time, locally defined coefficient [*Verruijt*, 1969]. Non-locality is well known for Darcy’s law, where flux behavior at a point depends not only on local permeability, but also on whether such point is well connected to the rest of the aquifer [*Renard and De Marsily*, 1997; *Sanchez-Vila et al.*, 2006]. Ironically, connectivity and Darcy’s flux non-locality affect field estimates of storage coefficient by accelerating or delaying the drawdown response to pumping [*Meier et al.*, 1998; *Sanchez-Vila et al.*, 1999]. Poroelasticity implies that storage behavior at a point depends not only on local elasticity properties, but also on deformations throughout the aquifer. Thus, both flux (because of heterogeneity) and storage (because of coupled deformation) at any point depend on heads elsewhere and are, thus, non-local. Therefore, if storage behavior would have to be represented by a simple parameter, this parameter would have to be function of space and time [*Narasimhan and Kanehiro*, 1980; *Murdoch and Germanovich*, 2012]. Injection (or pumping) exerts a force over the whole system that causes volumetric deformation and stress redistribution everywhere. In fact, field observations [*Verruijt*, 1969] and numerical studies [*Hsieh*, 1996; *Yin et al.*, 2007; *Berg et al.*, 2011] highlight that the presence of adjacent strata influence the deformation and therefore the pressure response, especially in the case of highly compressible media.

Treating storage as a constant-in-time and locally-defined parameter allows simplifying the flow equation into a linear diffusion equation, which is relatively easy to solve,

whereas acknowledging HM coupling requires numerical solution, which hinders its application. Therefore, the question is whether coupling effects are relevant. The objective of our work is to provide a deeper understanding of the HM pressure response and how to represent storage in the flow equation, especially with regard to boundary effects. To this end, we first revise the various definitions of specific storage as a property and then analyze the non-local nature of the storage behavior by means of analytic solutions to the HM problem of flow injection into one-dimensional and cylindrical two-dimensional laterally finite aquifers. These solutions highlight that the storage term in the fluid conservation equation becomes non-local (i.e., the storage term at a point depends on heads elsewhere) when the two-way HM coupling is acknowledged. This implies that the response in pressure would be different from what predicted by traditional methods.

2 Storage in deformable porous media

2.1 Local storage

Water released by a porous medium in response to a drop in pressure comes from (1) the expansion of water, characterized by its compressibility, β, (2) the growth of grains volume, characterized by the compressibility of the solid grains, $(1/Ks)$, and (3) the reduction in porosity associated to the rearrangement of grains and driven by the increase in effective compressive stress, characterized by the porous matrix compressibility, α. Therefore, it is most natural to write the specific storage coefficient as [*de Marsily*, 1981]

$$S_s = \phi\beta + \frac{1-\phi}{K_s} + \alpha \quad , \tag{1}$$

where ϕ is porosity. Note that the right hand side of Eq. (1) is usually multiplied by ρg (where ρ is fluid density and g is the acceleration of gravity), to express the response to change in head. However, we will be working with pressure. $1/Ks$ is usually much smaller than β or α, so that $(1-\phi)/K_s$ is normally neglected. The compressibilities of water and solid grains are local by definition. Difficulties arise with the compressibility of the porous matrix α because it is defined in terms of effective stresses and only indirectly related to head fluctuations, so that further assumptions are required. In order to properly define α, we have to introduce the Hooke's law of elasticity, which relates stresses and strains

$$\boldsymbol{\sigma}' = 2G\,\boldsymbol{\varepsilon} + \lambda\,\varepsilon_{vol}\,\mathbf{I} \quad , \tag{2}$$

where $\boldsymbol{\sigma}'$ is the change in effective stress tensor, $G = E/(2(1+\nu))$ and $\lambda = E\nu/((1+\nu)(1-2\nu))$ are the shear and Lamé moduli, respectively, E is Young's modulus, ν is Poisson ratio, $\mathbf{I}$ is the identity matrix, $\boldsymbol{\varepsilon} = 1/2\left[\nabla\mathbf{u} + (\nabla\mathbf{u})^T\right]$ is the strain tensor, $\varepsilon_{vol} = \nabla\cdot\mathbf{u}$ is the volumetric strain and $\mathbf{u}$ is the displacements vector. According to Eq. (2), it is easy to express the compressibility (α_σ) against mean effective stress σ'_m as

$$\alpha_\sigma = \frac{\varepsilon_{vol}}{\sigma'_m} = \frac{3}{2G+3\lambda} = \frac{1}{K} \quad . \tag{3}$$

This expression for compressibility is also valid under conditions of plane strain or uniaxial strain (i.e., $\varepsilon_i = 0$).

Actually, instead of α_σ, the compressibility against pressure α_p (i.e., volumetric deformation caused per unit change in water pressure) is usually introduced in Eq. (1). To this end, poroelasticity must be considered to relate variation of effective stress to variation of pressure, according to $\boldsymbol{\sigma}' = \boldsymbol{\sigma} + bp\mathbf{I}$, where $b = 1-(K/K_s)$ is the Biot-Willis coefficient with K representing the bulk modulus of the matrix, $\boldsymbol{\sigma}$ is the total stress tensor and tensile stress is assumed positive. The compressibility against pressure can be derived by assuming that effective stress changes equal bp in the directions along which the medium is free to deform, which leads to a general α_{p_n} of the form

$$\alpha_{p_n} = \frac{\varepsilon_{vol}}{p} = \frac{b}{2G/n+\lambda} \quad , \tag{4}$$

where n is the number of non-zero strain directions, or rather, the number of directions in which total stress is assumed to remain unchanged. It is easily verified that compressibility against pressure is equivalent to compressibility against stress (i.e., $\alpha_p = \alpha_\sigma$) when total stress remain unchanged in the three directions ($n = 3$) because b is often assumed to be 1. On the other hand, in the case of uniaxial strain, the definition of specific storage involves α_{p1}, which corresponds to the traditional Jacob's [*Jacob*, 1940] definition that assumes exclusively vertical deformation and no change in vertical total stress (i.e., $\sigma_z = 0; \varepsilon_x = \varepsilon_y = 0$).

2.2 Non-local storage

In the previous section we derived the compressibility against pressure by assuming zero total stress variation. However, this assumption may not be valid and the full HM problem has to be solved. The problem involves fluid mass conservation [*Coussy*, 2004]

$$\beta_T \frac{\partial p}{\partial t} + b\frac{\partial \varepsilon_{vol}}{\partial t} = \nabla\,\frac{k}{\mu}\nabla p\,, \tag{5}$$

where $\beta_T = \phi\beta + (b-\phi)/K_s$, where k is intrinsic permeability and μ is fluid viscosity. Note that β_T results slightly different from the corresponding term $S_\epsilon = \phi\beta + b/K_s - \phi/K_\phi$ in *Wang* [2000], where the unjacketed pore compressibility K_ϕ is equal to K_s only if the solid phase is composed of a single constituent [*Wang*, 2000].

Also, mechanical equilibrium is required, which, together with constitutive laws (e.g., Hooke's and Biot's law), yields [*Jaeger et al.*, 2007]

$$G\,\nabla^2\mathbf{u} + (G+\lambda)\;\nabla\left(\nabla\cdot\mathbf{u}\right) = \nabla\left(bp\right)\;. \tag{6}$$

These two equations have to be solved together with appropriate boundary and initial conditions. It is useful to reduce the system of Eq. (6) to one equation, by applying the divergence operator [*Verruijt*, 1969], which gives

$$(2G+\lambda)\nabla^2\varepsilon_{vol} = b\nabla^2 p\,. \tag{7}$$

where b has been considered homogeneous for simplicity.

Integration of the latter gives

$$(2G+\lambda)\varepsilon_{vol} = bp + f \quad , \tag{8}$$

where $f(\mathbf{x},t)$ is a harmonic function (i.e., such that $\nabla^2 f = 0$). In general, calculating f requires solving the fully coupled HM problem, as f depends on the shape and dimension of the medium and on the boundary conditions [*Gambolati*, 1974]. If the problem is uncoupled, by assuming constant total stress as in Section 2.1, the expression for f can be derived by comparing Eqs. (8) and (4), which leads to

$$f = \Big[(2G+\lambda)\alpha_{p_n} - b\Big]p = \frac{(n-1)(1-2\nu)}{1+(n-2)\nu}\;bp\;. \tag{9}$$

However, here we want to acknowledge the fully coupled HM behavior and keep (8) for f, which we use to express ε_{vol} in (5), yielding

$$\left(\beta_T + \frac{b^2}{2G+\lambda}\right)\frac{\partial p}{\partial t} + \frac{b}{2G+\lambda}\;\frac{\partial f}{\partial t} = \nabla\,\frac{k}{\mu}\nabla p\,, \tag{10}$$

where the temporal derivative of f is part of the storage term and determines its non-locality. Therefore, the storage term results different from the form adopted in the classical groundwater hydrology (Eq. (1)). This alteration should be considered if two-way hydro-mechanical coupling is analyzed.

Furthermore, in terms of mean stress, volumetric deformation is defined by $\varepsilon_{vol} = \alpha_\sigma(\sigma_m + bp)$, which can be substituted into Eq. (5) yielding

$$\left(\beta_T + b^2\alpha_\sigma\right)\frac{\partial p}{\partial t} + b\alpha_\sigma\frac{\partial \sigma_m}{\partial t} = \nabla\,\frac{k}{\mu}\nabla p\ . \tag{11}$$

If this latter equation is compared to Eq. (10), it can be again derived that f depends on the geometry (in order to transform $b/(2G+\lambda)$ into α_σ (Eq. (3)) and on the total stress variation, which may depend not only on the mechanical boundary conditions (restraints), but also on the distribution of the perturbation. Note that the expression $b\alpha_\sigma/(\beta_T + b^2\alpha_\sigma)$ defines the Skempton coefficient B [*Detournay and Cheng*, 1993; *Rice and Cleary*, 1976; *Zimmerman*, 2000], which relates the variation of pressure with the variation of total stress under undrained condition (i.e., $p = B\sigma_m$).

Eq. (10) is not very satisfying, because parameter f is unknown. We consider below some simple cases that allow us to define f without loosing the full HM coupling and thus allow us to gain insight into the variable, and non-local, nature of the storage behavior. In particular, we consider continuous injection into homogeneous and finite cylindrical and one-dimensional domains. Other cases can be solved by means of the proposed methodology.

3 One-dimensional finite domain

We first analyze the simplest case of unidirectional (linear) flow within a finite domain of dimension L with displacements allowed only in the flow direction $0 < x < L$, i.e., $\varepsilon_y = \varepsilon_z = 0$ and $\partial p/\partial y = \partial p/\partial z = 0$. It can be shown (Appendix A:) that the volumetric strains ($\varepsilon_{vol} = \varepsilon_x$) for constrained displacement at $x = 0$ and $x = L$ is expressed by

$$\varepsilon_{vol}(x,t) = \frac{b}{2G+\lambda}\left[p(x,t) - \frac{1}{L}\int_0^L p(x,t)dx\right] = \frac{b}{2G+\lambda}\left[p(x,t) - \overline{p}(t)\right], \tag{12}$$

where $\overline{p}$ indicates the spatial average of pressure. Therefore fluid mass conservation becomes

$$\left(\beta_T + b\alpha_{p1}\right)\frac{\partial p(x,t)}{\partial t} - b\alpha_{p1}\,\frac{\partial\,\overline{p}(t)}{\partial t} = \frac{k}{\mu}\,\frac{\partial^2 p(x,t)}{\partial x^2}\,, \tag{13}$$

where we have substituted $b/(2G+\lambda)$ with α_{p1}, defined in Eq. (4).

Comparing this equation to Eq. (10) yields that f is given by the spatial average of pressure, i.e., $f = -b\overline{p}(t)$. Therefore, the storage term is not just proportional to the local pressure fluctuations, but also to the mean pressure fluctuation along the whole domain.

To solve Eq. (13), we define

$$p^*(x,t) = p(x,t) + \theta\,\overline{p}\,(t) \quad , \tag{14a}$$

$$S_{s_1} = \beta_T + b\alpha_{p1} \quad , \tag{14b}$$

$$\theta = -\frac{b\alpha_{p1}}{S_{s_1}} \quad , \tag{14c}$$

$$D = \frac{k/\mu}{S_{s_1}} \quad . \tag{14d}$$

Using p^* and recognizing that the gradient of the spatial average is zero, Eq. (13) can be written as

$$\frac{\partial p^*(x,t)}{\partial t} = D\,\nabla^2 p^*(x,t)\,. \tag{15}$$

This equation is identical to the traditional flow equation, which can be solved for different problems [e.g., *Carslaw and Jaeger*, 1959]. The boundary condition for $p^*(x,t)$ is the same as for $p(x,t)$ at the injection point $x = 0$, where q_0 is injected, though not at the outer boundary $x = L$. The solution in terms of pressure can then be found by means of Eq. (14a), where $\overline{p}(t)$ depends on the hydraulic boundary conditions at the outer boundary.

3.1 Constant pressure at the outer boundary

In this case, the boundary condition at the outer boundary is

$$p^*(L,t) = \theta\,\overline{p}(t)\,, \tag{16}$$

which is inconvenient because it depends on the solution. Instead, we obtain a supplementary condition by evaluating the spatial average of p^*, as given by Eq. (14a)

$$\overline{p^*}(t) = \frac{1}{L}\int_0^L p^*(x,t)dx = (1+\theta)\,\overline{p}(t) = \frac{1+\theta}{\theta}\,p^*(L,t)\,. \tag{17}$$

Once p^* solution is obtained (Appendix B:), Eqs. (14a) and (16) lead to

$$p(x,t) = p^*(x,t) - p^*(L,t)\,, \tag{18}$$

which allows us to define the solution to the problem in terms of p (Appendix B:).

The problem can be greatly simplified if the compressibility of solid grains and water, β_T, is assumed much smaller than the compressibility of the porous medium and neglected, so that $\theta = -1$ and $D = (k/\mu)/\alpha_{p1}$, where Biot-Willis coefficient b has been taken

equal to 1, neglecting solid grains compressibility [*Detournay and Cheng*, 1993]. With these assumptions, valid for unconsolidated soils but not for stiff rocks, p^* simply represents the fluctuation with respect to the spatial average, i.e., $p(x,t) = \overline{p}(t) + p^*(x,t)$, and the supplementary condition (Eq. (17)) becomes

$$\frac{1}{L}\int_0^L p^*(x,t)dx = 0\,, \tag{19}$$

which is logical, because the spatial average of the fluctuation is zero by definition.

After solving for p^* (Appendix B:) and application of Eq. (18), the solution for $p(x,t)$ becomes:

$$p(x,L,t) = p_{trad}(x,L/2,t) + \overline{p}(t) \quad , \tag{20}$$

where $p_{trad}(x,t)$ is the well-known solution to the traditional (i.e., without HM coupling) problem of 1-D injection into a finite domain [*Carslaw and Jaeger*, 1959]

$$p_{trad}(x,L,t) = \frac{q_0}{k/\mu}\sqrt{4Dt}\sum_{m=0}^{\infty}(-1)^m\Big[A(2L,x) - A(2L,2L-x)\Big]\,, \tag{21}$$

whereas

$$\overline{p}(t) = p_{trad}(0,L/2,t) \quad , \tag{22}$$

with $A(\Gamma,\psi) = \text{ierfc}\left[(\Gamma m + \psi)/\sqrt{4Dt}\right]$ and ierfc indicates the integral error function, defined as $\text{ierfc}(y) = \exp(-y^2)/\sqrt{\pi} - y\,\text{erfc}(y)$. This series converges very fast because it is alternate and because the exponential term in A decays rapidly as m increases. This is especially true for small time, but truncation at $m = 2$ is sufficient even for large time, as shown by comparison with numerical solutions (Fig. 1).

The HM solution corresponds to the traditional solution for half the domain plus the spatial average of pressure $\overline{p}$, given by the traditional solution for half the domain at $x = 0$. At early time ($t < 0.1t_c$, where $t_c = L^2/D$ is the characteristic time of the problem) the extension of the domain is not relevant, thus the HM effects implies raising pressure by a constant ($\overline{p}$) within the whole domain, except near the outer boundary, where pressure was prescribed to be zero (Figs. 1 and 2). Note that the drop in pressure, with respect to the constant $\overline{p}$, near this boundary is identically symmetric to the rise near the inflow (Fig. 1).

For time greater than $0.1t_c$, the outer boundary starts to significantly affect the solution within the whole domain. Thus, the difference between solutions is given not only by $\overline{p}$, but depends on the position, being greater in the vicinity of the injector and smaller in the vicinity of the constant pressure boundary (Fig. 2). At time greater than the charac-

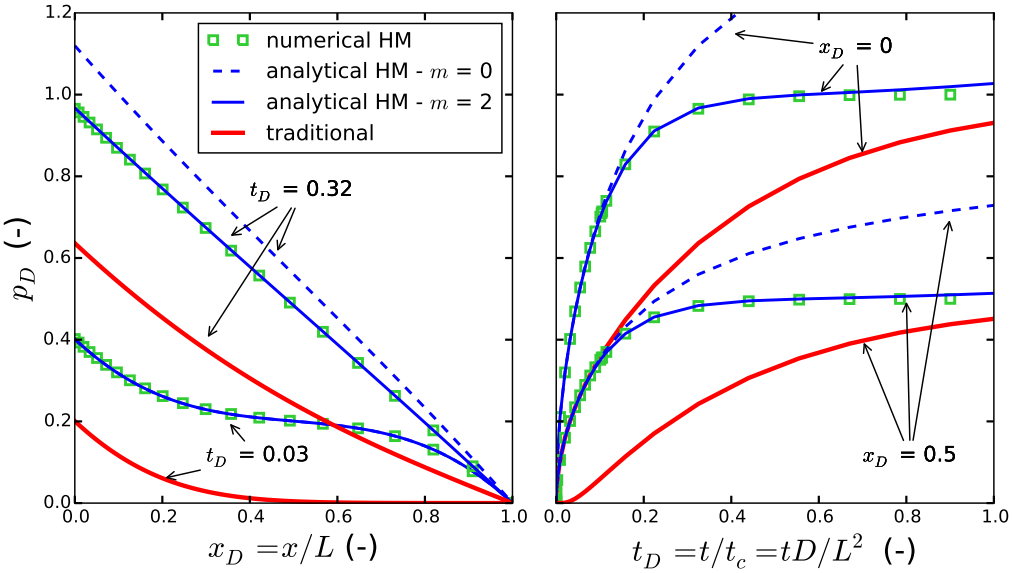

Figure 1. Comparison between traditional and hydromechanical solutions for the one-dimensional domain with constant pressure at the outer boundary. Also shown are the results of truncating the series after m=0 and m=2, against results of numerical simulations. Results are normalized with respect to $q_0 L\mu/k$, which is the steady state pressure at $x = 0$.

teristic time t_c the difference tends to zero, because both solutions tend to the steady state and the effect of pressure derivatives becomes negligible.

3.2 No flow at the outer boundary

When a no flow boundary condition is imposed at $x = L$, the problem in terms of p^* is subject to the same BCs than the traditional flow problem at both boundaries (Appendix B:). However, the value of the spatial average $\overline{p}$ is unknown. It can be found by operating the spatial average of Eq. (13), which gives

$$\beta_T \frac{\partial \overline{p}}{\partial t} = \frac{1}{L}\left(q_0 - q_L\right) , \tag{23}$$

where q_0 and q_L represents the flux at $x = 0$ and $x = L$, respectively.

This equation highlights that the spatial average of the water storage is exclusively due to the compressibility of water and solid grains (β_T), which therefore cannot be disregarded. This implies that parameter θ cannot be equal to -1. This simply reflects that if the medium cannot deform and fluid and grains are incompressible, fluid injection would

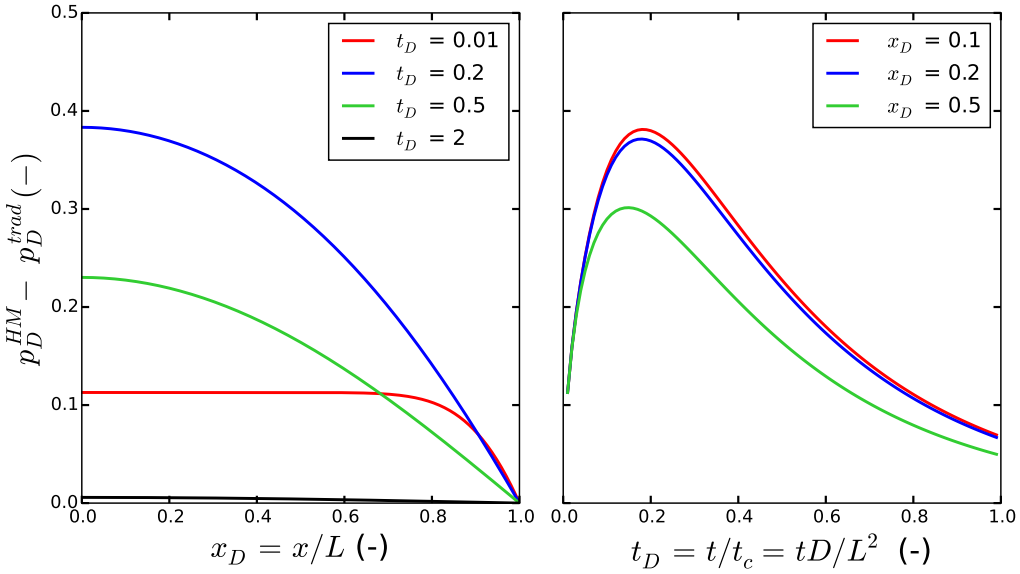

Figure 2. Difference between hydro-mechanical and traditional solutions ($p_D^{HM} - p_D^{trad}$) for the one-dimensional domain with constant pressure at the outer boundary. Results are normalized with respect to $q_0 L\mu/k$, which is the steady state pressure at $x = 0$.

cause an infinite pressure buildup. In our case, with constant q_0 and zero q_L, the spatial average is therefore defined by

$$\overline{p}(t) = \frac{q_0\, t}{\beta_T L}\,, \tag{24}$$

which allows to find the solution in terms of $p(x,t)$

$$p(x,t) = p_{trad} - \theta \frac{q_0\, t}{\beta_T L} \quad , \tag{25}$$

where p_{trad} is the traditional solution given by [*Carslaw and Jaeger*, 1959]

$$p_{trad}(x,t) = \frac{q_0}{k/\mu}\sqrt{4Dt}\sum_{m=0}^{\infty}\Big[A(2L,x) + A(2L,2L-x)\Big] \tag{26}$$

and $A(\Gamma,\psi)$ has been defined above.

Solution (25) can be normalized with respect to $q_0 L\mu/k$, which, together with eqs. (14c) and (14d), gives

$$p_D(x,t) = p_{trad_D}(x,t) + \frac{b\alpha_{p1}}{\beta_T}\, t_D \tag{27}$$

where p_D and p_{trad_D} are the dimensionless form of p and p_{trad} and $t_D = tD/L^2$. This expression highlight that the term $b\alpha_{p1}/\beta_T$ is the governing dimensionless parameter for the case of no flow at the outer boundary.

Figure 3 displays the comparison between the traditional and the HM solutions, whose validity is tested against numerical solutions. It is clear that the two solutions diverge by the spatial average $\overline{p}$, which is constant in space and increases linearly with time and with the parameter $b\alpha_{p1}/\beta_T$. This latter parameter is assumed approximately equal to 150 in this example, which means that θ is slightly smaller than 1.

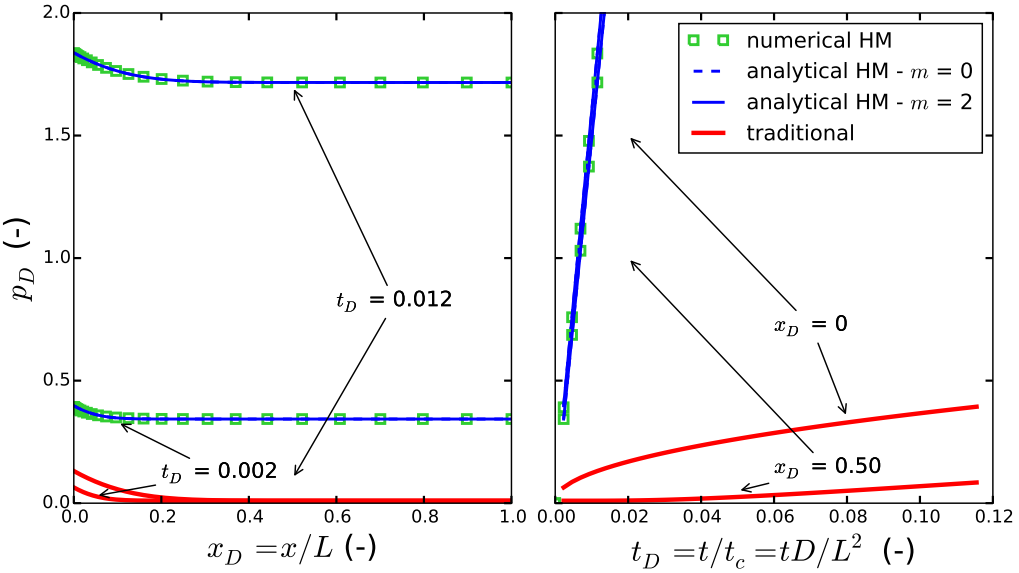

Figure 3. Comparison between traditional and hydromechanical solutions for the one-dimensional domain with no flow outer boundary. Also shown are the results of truncating the series after *m*=0 and *m*=2, against results of numerical simulations. Results are normalized with respect to $q_0 L\mu/k$.

4 Cylindrical finite domain

We now consider the more general case of radial flow within a finite aquifer $r_0 < r < R$, adopting cylindrical coordinates r, θ, z and axial symmetry around the z-axis. For the sake of simplicity, we consider the cases of plane strain or plane stress in the z direction, i.e., $\varepsilon_z = 0$ and $\sigma_z = \tau_{rz} = \tau_{\theta z} = 0$, respectively. The former may correspond to an aquifer with infinite extension in the z direction. The latter represents a thin aquifer confined between two soft layers, which cannot resist shear stress [*Verruijt*, 1969].

The expression for the volumetric strains, for both plane stress and plane strain, is (Appendix C:)

$$\varepsilon_{vol} = \alpha_{p_n} \left[p(r,t) + g_1 \, 2C(t) \right] \quad , \tag{28}$$

where g_1 is 1 for plane strain and $(1-2\nu)/2/(1-\nu)$ for plane stress and α_{p_n} is the compressibility against pressure (Eq. (4)) with n=1 for plane strain and n=2 for plane stress. The latter may surprise because n was defined as the number of non-zero strain directions (which is actually 2 for plane strain and 3 for plane stress) or the number of directions along which total stress does not change (0 for plane strain, 1 for plane stress). In reality, Eq. (4) was derived by assuming that either strain or total stress were zero along three orthogonal directions, a condition that is not met in this case. The actual α_{p_n} are derived from the axial symmetry assumption and the equilibrium equations (Appendix C:). In the resulting α_{p_n}, however, n corresponds to the number of non-zero displacements, rather than to the non-zero strains.

Constant C is zero for infinite aquifer, but depends on the mechanical boundary conditions for finite domain. We consider zero displacements ($u_r = 0$) or prescribed stress (σ_r) at the inner and outer radius $r = r_0$ and $r = R$, which results in 4 scenarios. They lead to different expressions for the constant C that, in the case of small inner radius r_0, are mostly dependent on the outer BC and can be summarized as

$$C = \frac{g_2}{R^2}\int_{r_0}^{R} r p(r,t) dr = \frac{g_2\,\overline{p}(t)}{2} \quad , \tag{29}$$

where g_2 is -1 (both plane stress and plane strain) for zero lateral displacements at the outer boundary and $(1-\nu)/(1+\nu)$ (plane stress) or $1-2\nu$ (plane strain) for zero increase in total stress at the outer boundary, as shown in Appendix C: .

Therefore, fluid mass conservation (Eq. (10)) is expressed by

$$\left(\beta_T + b\alpha_{p_n}\right)\frac{\partial p(x,t)}{\partial t} + b\alpha_{p_n} g_1\, g_2\, \frac{\partial \overline{p}(t)}{\partial t} = \frac{k}{\mu}\,\frac{1}{r}\,\frac{\partial}{\partial r}\left(r\frac{\partial p(r,t)}{\partial r}\right), \tag{30}$$

which shows again the non-local nature of the storage term. Similarly to the one-dimensional case, we define

$$p^*(r,t) = p(r,t) + \theta\,\overline{p}(t) \quad , \tag{31a}$$

$$S_{s_r} = \beta_T + b\alpha_{p_n} \quad , \tag{31b}$$

$$\theta = \frac{b\alpha_{p_n} g_1 g_2}{S_{s_r}} \quad , \tag{31c}$$

$$D = \frac{k/\mu}{S_{s_r}} \quad , \tag{31d}$$

which allows us to transform Eq. (30) into the well-known diffusion equation in radial coordinates

$$\frac{\partial p^*(r,t)}{\partial t} = D\,\frac{1}{r}\,\frac{\partial}{\partial r}\left(r\,\frac{\partial p^*(r,t)}{\partial r}\right)\,. \tag{32}$$

The boundary conditions for this problem are identical to the ones of the traditional flow problem at the injection boundary $r = r_0$, where Q_0 is injected, but differ at the outer boundary $r = R$.

4.1 Constant pressure at the outer boundary

As for the one-dimensional case, given the inefficiency of the outer BC

$$p^*(R,t) = \theta\,\overline{p}(t)\,, \tag{33}$$

we define a supplementary condition by spatial averaging p^* in Eq. (31a), which yields

$$\overline{p^*}(t) = \frac{2}{R^2 - r_0^2}\int_{r_0}^{R} r\,p^*(r,t)dr = (1+\theta)\,\overline{p}(t) = \frac{1+\theta}{\theta}\,p^*(R,t)\,. \tag{34}$$

Once p^* has been found (Appendix D:), Eqs. (31a) and (33) lead to

$$p(r,t) = p^*(r,t) - p^*(R,t)\,, \tag{35}$$

which allow us to define the solution in terms of p in the Laplace domain

$$\widehat{p}(r,s) = C_1\Big[I_0(r\eta) - I_0(R\eta)\Big] - \frac{2}{\pi}C_2\Big[K_0(r\eta) - K_0(R\eta)\Big]\,, \tag{36}$$

where I_0 and K_0 represent the modified Bessel functions of first and second kind, respectively, of order zero, whereas $\eta = \sqrt{s/D}$, with s representing the Laplace variable. Constants C_1 and C_2 depend on the hydraulic and mechanical boundary conditions, as well as on the condition on strain or stress in the z direction (Appendix D:).

Again, the problem can be greatly simplified disregarding the compressibility of water and solid grains, β_T, with respect to the compressibility of the porous medium, which also implies $b = 1$. In this case, the values of the parameter θ and D are the ones given in Table 1.

In the simpler case of plane strain and zero displacement at the outer boundary, $p^*(r,t)$ represents the fluctuation of pressure with respect to the spatial average, i.e., $p(r,t) = \overline{p}(t) + p^*(r,t)$. Therefore the supplementary condition (Eq. (34)) becomes $\overline{p^*}(t) = 0$, which is logical, since the spatial average of the fluctuation is zero by definition.

Table 1. Values of parameters θ and D when compressibilities of solid grains and water are disregarded. Values of θ depend on the mechanical BC at the outer radius, which can be of zero displacement (constrained) or zero total stress (unconstrained).

		Plane stress	**Plane strain**
D		$\frac{k/\mu}{1/(G+\lambda)}$	$\frac{k/\mu}{1/(2G+\lambda)}$
θ	**Constrained**	$-\frac{1-2\nu}{2(1-\nu)}$	-1
	Unconstrained	$\frac{1-2\nu}{2(1+\nu)}$	$1-2\nu$

In this case the solution for pressure in the Laplace domain is

$$\widehat{p}(r,s) = \frac{Q_0}{2\pi k/\mu}\,\frac{1}{s}\left\{\frac{RK_1(R\eta) - r_0K_1(r_0\eta)}{RI_1(R\eta) - r_0I_1(r_0\eta)}\left[I_0(r\eta) - I_0(R\eta)\right] + K_0(r\eta) - K_0(R\eta)\right\}, \tag{37}$$

where I_m and K_m are modified Bessel's functions of first and second kind, of order m, respectively.

Instead, the solution to the conventional problem in the Laplace domain is given by [*Carslaw and Jaeger*, 1959; *Chen*, 1984; *Verruijt*, 2013]

$$\widehat{p}_{trad}(r,s) = \frac{Q_0}{2\pi k/\mu}\,\frac{1}{s}\left[-\frac{K_0(R\eta)}{I_0(R\eta)}\,I_0(r\eta) + K_0(r\eta)\right]. \tag{38}$$

Numerical inversion of this Laplace transform solution is compared with results of discrete finite element numerical simulators (Code_Bright [*Olivella et al.*, 1994, 1996] and an application of Kratos Multiphysics [*Gómez-Castro et al.*, 2015; *Dadvand et al.*, 2010; *CIMNE*, 2012]) and with the traditional solution in Fig. 4.

The behavior is similar to the one-dimensional case (Fig. 2) in that pressure builds up immediately throughout the domain due to the horizontal stress caused by the push of injected water, although the understanding of the analytic expressions is less intuitive.

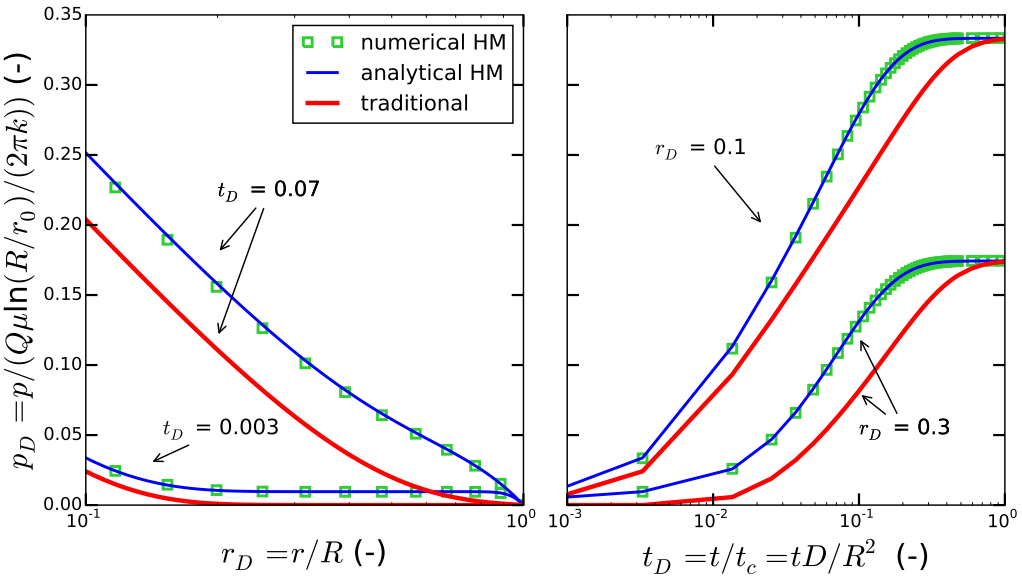

Figure 4. Comparison between traditional and hydromechanical solutions for the cylindrical domain with constant pressure outer boundary, plane strain and zero displacement at the inner and outer boundaries. Also shown are the results of numerical simulations. Pressures are normalized with respect to $Q_0\mu \ln(R/r_0)/(2\pi k)$, which is the steady state pressure at $r = r_0$.

For early times ($t < 0.1t_c$, with $t_c = R^2/D$), the traditional solution is Theis' (i.e., response for infinite domain, as the outer boundary condition does not yet affect pressures). The HM overpressure is larger by the same amount ($\overline{p}$) over the domain, except near the outer boundary (Fig. 5). For times greater than 0.1 t_c, the difference between solutions varies with space, being greatest near the injector. This behavior is consequence of the outer boundary prescribed pressure, which tends to reduce the pressure increase. In fact, the deviation respect to the traditional solution is maximum at around $t = 0.2t_c$. For time greater than t_c, both solutions converge to the steady state (Thiem) solution.

The pressure field predicted by the HM solution is different from the traditional one also when the outer boundary is free to deform (Fig. 6). The deviation is smaller than in the constrained case and it is negative because the medium deforms more than calculated by means of compressibility, as also expressed by Eqs. (28) and (29). The negative deviation is quite surprising because it implies that injection may cause a drop in pressure. Actually, the drop only occurs ahead of the injection pressure cone and reflects that, since radial displacements are unhindered, the medium tends to expand laterally by the

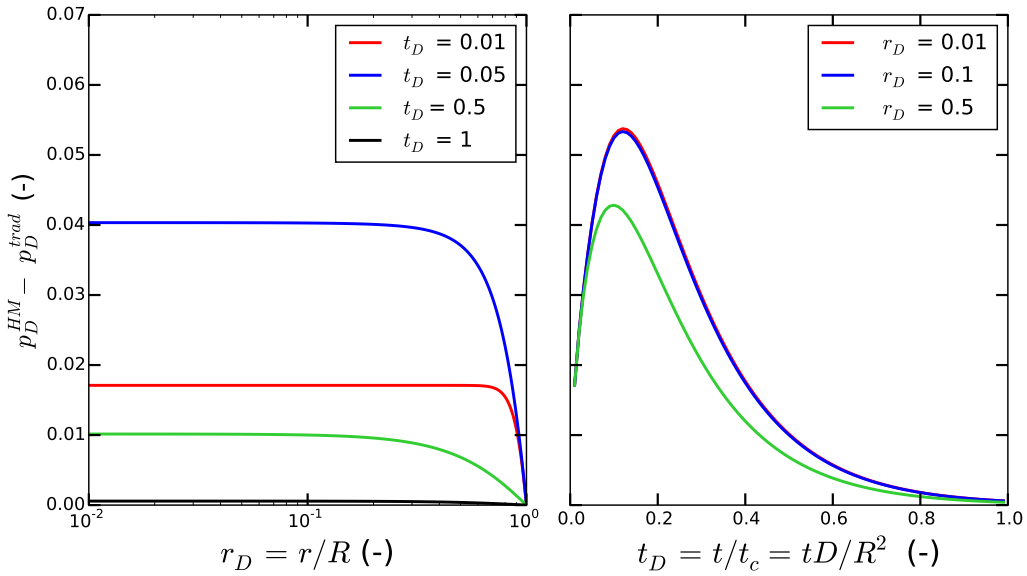

Figure 5. Difference between hydro-mechanical and traditional solutions ($p_D^{HM} - p_D^{trad}$) for the cylindrical domain in plane strain with constrained outer boundary. Results are normalized with respect to $Q_0\mu \ln(R/r_0)/(2\pi k)$, which is the steady state pressure at $r = r_0$. A value of 0.3 is assumed for the Poisson's ratio.

push of water near the injection point. A similar drop in pressure has been observed during interference slug tests at the Clemson well field, as reported by *Slack et al.* [2013], who attribute the effect to a non-local opening of fractures due to the pressure increase. A very similar drop was observed during hydraulic stimulation of the EGS Camborne project [*Batchelor*, 1983], who also attributed it to dilation of joints unconnected to the "main flow system". Without discarding dilation, our findings imply that lateral expansion can explain reverse pressure fluctuation whenever radial deformation is allowed. The behavior is different from other reverse water-level fluctuations, such as the Noordbergum effect [*Verruijt*, 1969] and the Rhade effect [*Langguth and Treskatis*, 1989], which occur in confining strata adjacent to the stimulated one.

The behavior in the case of plane stress (constrained and unconstrained cases) is similar to that observed for the plane strain, but scaled according to the values of parameter θ (Table 1), which are around 1/3 of the corresponding plane strain θ. A comparison between the two cases is shown in Supplementary Information.

In general, the deviation respect to the traditional solution is largest in the case of plane strain with constrained outer boundary, whereas it is smallest but reverse in the case of plane stress with unconstrained outer border. This result reflects that the HM additional pressure variation is inversely proportional to the possibility of the medium to deform. In general, HM coupling can be disregarded when the medium is free to deform.

4.2 No flow at the outer boundary

The case of no flow at the outer boundary is similar to the one-dimensional case in that the solution for p^* is completely defined by the BCs and corresponds to the traditional solution of the hydraulic problem p_{trad} (Appendix D:). To find the HM solution in terms of pressure, the spatial average $\overline{p}$ is obtained by averaging Eq. (30) and taking into account Eqs. (31), which yields

$$S_{s_r}\,(1+\theta)\,\frac{\partial \overline{p}}{\partial t} = \frac{Q_0 - Q_R}{\pi(R^2 - r_0^2)}\,, \tag{39}$$

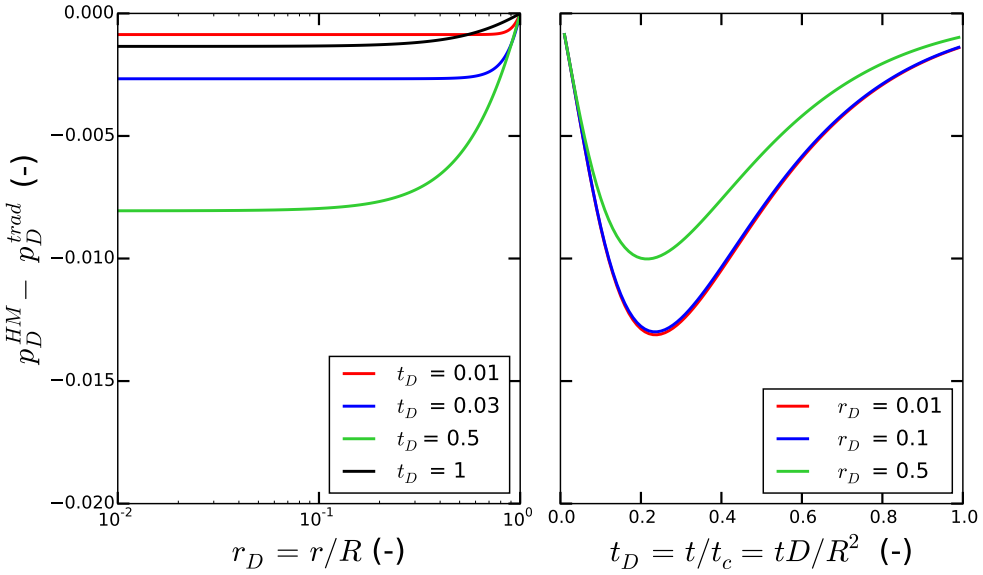

Figure 6. Difference between hydro-mechanical and traditional solutions ($p_D^{HM} - p_D^{trad}$) for the cylindrical domain in plane strain with unconstrained outer boundary. Results are normalized with respect to $Q_0\mu\ln(R/r_0)/(2\pi k)$, which is the steady state pressure at $r = r_0$. A value of 0.3 is assumed for the Poisson's ratio.

where Q_0 and Q_R represent the inflow at $r = r_0$ and the outflow at $r = R$, respectively. In our case, with constant Q_0 and zero Q_R, the spatial average is

$$\overline{p}(t) = \frac{1}{S_{s_r}\,(1+\theta)}\;\frac{Q_0\,t}{\pi(R^2 - r_0^2)}\;. \tag{40}$$

Introducing Eq. (40) into Eq. (31a) returns the HM solution for pressure, which normalized with respect to $Q_0\mu/(\pi k)$ and taking into account Eq. (31d), becomes

$$p_D = p_{trad_D} - \frac{\theta}{1+\theta}\,t_D\;, \tag{41}$$

where $t_D = tD/(R^2 - r_0^2)$ and p_D and p_{trad_D} are the dimensionless expressions of p and p_{trad}. It is clear that the dimensionless term $-\theta/(1+\theta)$ governs the discrepancy between traditional and HM solutions. In the plane strain case with constrained outer boundary this parameter corresponds to $b\alpha_{p_1}/\beta_T$, like in the case of one-dimensional domain. Note that the values of θ given in Table 1 do not apply to this case, in which we cannot disregard β_T.

The solution to the traditional problem is given in the Laplace space by [*Carslaw and Jaeger*, 1959]

$$\widehat{p}_{trad}(r,s) = \frac{Q_0}{2\pi k/\mu}\;\frac{1}{s}\left[\frac{K_1(R\eta)}{I_1(R\eta)}I_0(r\eta) + K_0(r\eta)\right]\;. \tag{42}$$

Therefore the solution in terms of pressure can be written in the Laplace domain as (Appendix D:)

$$\widehat{p}(r,s) = \widehat{p}_{trad}(r,s) + \frac{1}{S_{s_r}\,(1+\theta)}\;\frac{Q_0}{\pi(R^2 - r_0^2)}\;\frac{1}{s^2}\;. \tag{43}$$

Similar to the one-dimensional domain, it is apparent that the two solutions diverge by the spatial average $\overline{p}$, which is constant in space and increases linearly with time (Eq. (40)). Therefore, when long-term continuous injection is performed in bounded aquifer, ignoring the HM coupling implies a great underestimation of the pressure variation.

5 Sensitivity to parameters

HM coupling acknowledges that pressure gradients imply a load that produces deformations throughout the flow domain and causes a deviation with respect to the hydraulic solution because storage is modified respect to the traditional formulation by an amount proportional to the spatial average $\overline{p}$ (Eqs. (13) and (30)). The deviation tends to increase with time and to reduce with the domain dimension (Eqs. (24) and (40)). However, $\overline{p}$ is strongly affected by the boundary conditions.

In the case the outer BC is of no flow, the deviation from the traditional solution increases with time and decreases with the domain extension, as apparent in Eqs. (25) and (43).

The behavior is different and more complex in the case of prescribed pressure at the outer boundary, which limits the increase of pressure, and therefore of $\overline{p}$. Figure 7 displays pressure evolution for three values of the domain extent for the one-dimensional (upper) and the cylindrical (lower) domains in both dimensional (left) and dimensionless (right) variables. This allows us to get a double point of view, because the dimensional scale exhibits the behavior as it would be observed, while the dimensionless scale reveals the actual dependence on the domain extent, which is however unknown in real situations.

In the case of one-dimensional domain, the deviation is independent on the domain extent at early times, whereas it increases significantly with L for greater times (Fig. 7a). When results are scaled with the respective characteristic pressure and time (Fig. 7b), the curves collapse and the peak occurs at dimensionless time t_D=0.2, which shows that the deviation is proportional to the domain dimension.

The behavior is significantly different in the cylindrical domain (Fig. 7 - lower panels). The case of plane strain and constrained outer boundary is considered here, but we have observed that the behavior of the other cases is similar, but scaled according with values of parameter θ (Table 1). At early time, the deviation is greater for smaller domain extension R, but the peak values are pretty insensitive to domain extent, with an almost imperceptible increase for larger R (Fig. 7c). On the other hand, when results are normalized with the respective characteristic pressure and time (Fig. 7d), the peaks are greater for smaller domain, which is coherent with the tendency of the spatial average $\overline{p}$.

The influence of the outer boundary is slight in the cylindrical domain and great for one-dimensional domain. The reason for this discrepancy resides in the geometry, because the volume of aquifer affected increases with the square of the radius of the cone of overpressure in the cylindrical case, but only linearly in the one-dimensional case. The implications are interesting, since the domain extension is in general unknown. In the cylindrical domain, which is the most realistic, the maximum deviation is almost independent of the domain extension.

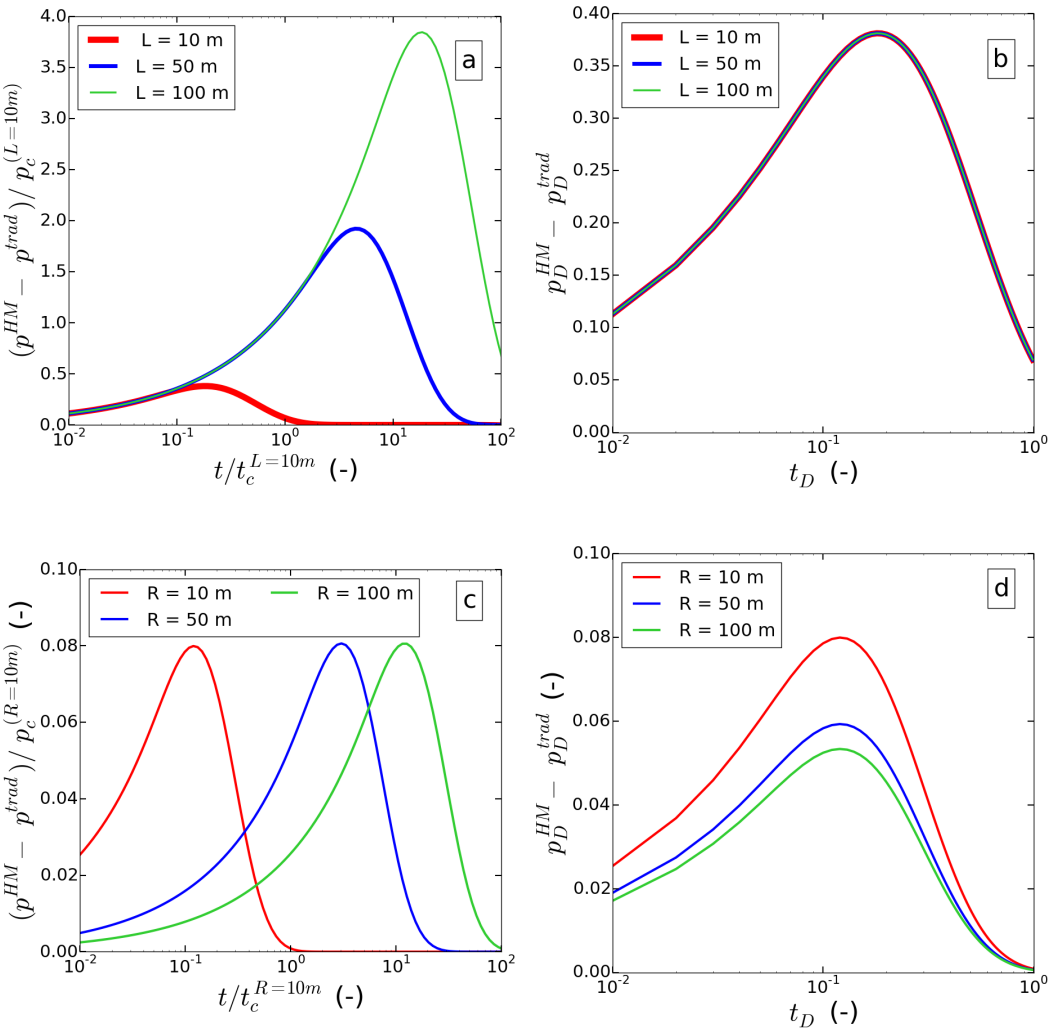

455 **Figure 7.** Time evolution of the difference between HM and traditional solutions ($p_D^{HM} - p_D^{trad}$) for one-
456 dimensional (above) and cylindrical (below) domain with plane strain and constrained outer boundary and
457 for three values of domain extension in both dimensional (a and c - pressure and time are scaled by a constant
458 value) and dimensionless variable (b and d). Results are relative to a point placed at 1 m distance from the
459 well (a and c) and at dimensionless distance equal to 0.1 (b and d).

In the foregoing we have simplified the solution to the problems with constant pressure at the outer boundary, disregarding the compressibility of solid grains and water with respect to that of the porous medium. This simplification is valid for unconsolidated aquifers, but not necessarily for rocks, especially at large depths. If the compressibility of grains and water (β_T) is acknowledged, the solution is barely sensitive to the compressibility of the porous matrix, which slightly modifies the parameter θ (Eqs. (14c) and (31c)), i.e., θ is smaller for stiffer rocks. Note that, when β_T is ignored, θ depends solely on Poisson's ratio, but not on the actual stiffness of the medium (Tab. 1).

Moreover, response is quite sensitive to compressibility of solid grains K_s, which is strictly related to the Biot-Willis coefficient b. It is often assumed that solid grains are incompressible, which corresponds to $b = 1$. However, b can be smaller than 1, especially in rocks [*Nur and Byerlee*, 1971; *Mitchell et al.*, 2005]. Smaller values of b corresponds to smaller θ (recall Eqs. (31c) and (4)), which reduces the difference between HM and traditional formulation in both cases of prescribed pressure (Fig. 8) and prescribed flux (Eq. (43)) on the outer boundary.

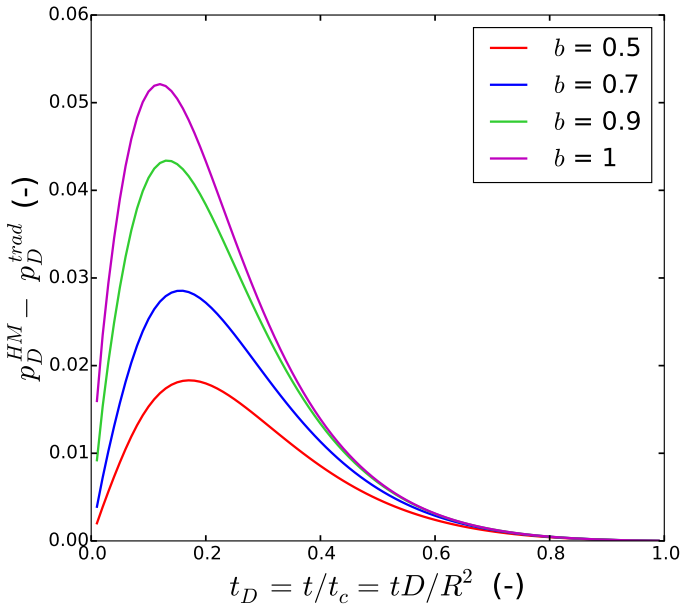

Figure 8. Sensitivity analysis respect to the Biot-Willis coefficient b for the case of cylindrical domain with plane strain and constrained outer boundary. Difference between HM and traditional solutions ($p_D^{HM} - p_D^{trad}$) vs dimensionless time for a point placed at 1 m distance from the well. Pressure is normalized with respect to the steady state pressure at $r = r_0$.

6 Discussion and Conclusions

Storage expresses the volumetric deformation capacity of the aquifer. The main point of our work is that deformation capacity depends not only on the compressibility of the medium, but also on the geometry of the aquifer and on the surrounding constraints to deformation, because hydraulic gradients act as body forces that press the medium in the direction of flow. We apply poroelasticity equations to highlight the non-local nature of the storage behavior, i.e., its dependence on the pressure distribution over the whole aquifer.

We present analytic solutions to the coupled hydro-mechanical problem of fluid injection (or extraction) into finite aquifers, i.e., aquifers that are laterally confined by surrounding formations. To acknowledge the two-way coupling we first derive the analytic expression for the deformations of the medium produced by pressure variations and then back-calculate the pressure response. Therefore, our results are identical to what would be obtained with fully coupled numerical simulations, but our analytic expressions provide a faster calculation and illustrate the scaling.

We analyze the HM pressure response and its deviation respect to the traditional hydraulic solutions, which allows us to gain understanding on the role of boundary effects, which is important because modellers often wonder about the right size of the domain. If the lateral confinement allows deformations, the deviation is small and may be disregarded, so that the classical storage coefficient can be adopted with a small error. Still, zero lateral confinement produces reverse pressure fluctuations, which we suspect should be expected whenever injection is produced in stiff portions of the massif. On the other hand, if the aquifer deformation is constrained by the surrounding formations, pressure variations may be greater than expected (i.e., calculated according to the traditional methods). These findings are useful for modelers to improve awareness about numerical HM simulations, but are also useful for prediction or interpretation of real problems. We have adopted the hypotheses of a complete restraint on the outer boundary, which may be not realistic. However, even a partial restraint of deformations may have significant effects on the pressure response. This correction should, therefore, be taken into account in situation of massive injection, such as Enhanced Geothermal Systems or CO_2 geological storage, because maximum sustainable pressure limit can be exceeded.

525 HM coupling also implies that the pressure response propagates faster than predicted
526 by the traditional solution, which upsets the concept of characteristic response time. This
527 complicates the estimation of the area affected by overpressure at certain time of injection,
528 which is an important parameter for safe operation of energy-related activities.

529 It is worth noting that the described behavior applies on both injection and pumping.
530 If the pumped aquifer is bounded by a rigid formation that hinders lateral displacements,
531 the estimation of the storage coefficient from field pumping tests leads to an overestima-
532 tion of the mechanical parameters [*Pujades et al.*, 2017], which will not correspond with
533 the results of laboratory tests.

534 Despite the strong idealization of the condition adopted here, we have shown that
535 the behavior is independent on the reservoir radial extension, thus the proposed solution
536 can be adopted in conjunction with the traditional methods in order to compare the re-
537 spective estimation of the hydraulic and mechanical parameters. In fact, we conjecture
538 that mechanical effects will be significant in low permeability (i.e., high overpressure for
539 a given flow rate), high stiffness media. Analyzing these media is becoming increasingly
540 relevant as numerous activities are being developed at great depth (CO_2 storage, Enhanced
541 Geothermal Systems, shale gas production or waste disposal).

542 Finally, the proposed solution also provides a solid benchmark for new fully coupled
543 HM codes, as it represents the two-way coupling better than the classical consolidation
544 problem (Terzaghi problem), which only represents the diffusive process. To facilitate this
545 task, a set of numerical results and the corresponding input data are provided as Supple-
546 mentary Information.

547 A: Volumetric deformation in one-dimensional domain

548 In the case of one-dimensional domain, the equilibrium equation in the x direction
549 results

$$\frac{\partial \sigma_x}{\partial x} = 0\,. \tag{A.1}$$

550 Application of Hooke's law [*Jaeger et al.*, 2007] yields

$$\frac{\partial^2 u_x}{\partial x^2} = \frac{b}{2G+\lambda}\,\frac{\partial p}{\partial x}\,, \tag{A.2}$$

where $b/(2G + \lambda)$ can be substituted with α_{p1}. This equation can be integrated to yield [*De Simone et al.*, 2017]

$$u_x = \alpha_{p1}\left[\int_0^x p(x,t)dx + Ax + B\right] \tag{A.3}$$

and the volumetric deformation is

$$\varepsilon_{vol} = \varepsilon_x = \frac{\partial u_x}{\partial x} = \alpha_{p1}\Big[p(x,t) + A\Big]\,, \tag{A.4}$$

where constants A and B depend on the mechanical BC at the surfaces $x = 0$ and $x = L$. In the case that displacements is constrained at both surfaces ($u = 0$), constants are expressed by

$$A = -\frac{1}{L}\int_0^L p(x,t)dx \tag{A.5}$$

$$B = 0 \quad . \tag{A.6}$$

B: HM Pressure solution in 1D domain

Laplace transform with respect to time of Eq. (15) yields

$$s\,\widehat{p^*}(x,s) = D\,\frac{\partial^2 \widehat{p^*}(x,s)}{\partial x^2}\,, \tag{B.1}$$

where s is the Laplace variable and the hat denotes the functions in Laplace space. The general solution is given by [*Carslaw and Jaeger*, 1959]

$$\widehat{p^*}(x,s) = C_1\exp(\eta x) + C_2\exp(-\eta x)\,, \tag{B.2}$$

where $\eta = \sqrt{s/D}$.

Constants C_1 and C_2 are defined by the BCs. Constant injection q_0 is applied at the inner boundary ($x = 0$), whereas for the outer boundary ($x = L$) we take into consideration two different boundary conditions, which are constant pressure and zero normal flow. In the case of constant pressure at the outer boundary $x = L$, the conditions are the ones defined in Section 3.1:

$$\begin{cases} \dfrac{\partial \widehat{p^*}(x,s)}{\partial x}\bigg|_{x=0} = -\dfrac{q_0}{k/\mu}\,\dfrac{1}{s} & \text{(B.3a)} \\[2ex] \displaystyle\int_0^L \widehat{p^*}(x,s)dx = \frac{1+\theta}{\theta}\,L\,\widehat{p^*}(L,s)\,. & \text{(B.3b)} \end{cases}$$

After deriving the expressions for C_1 and C_2 and applying Eq. (18), the expression of pressure in the Laplace domain is

$$\widehat{p}(x,s) = \frac{q_0}{k/\mu}\,\frac{1}{s\,\eta}\,\frac{\left[(1+\gamma)\,\mathrm{e}^{-\eta(L-x)} + (1-\gamma)\,\mathrm{e}^{\eta(L-x)} - \mathrm{e}^{\eta x} - \mathrm{e}^{-\eta x} + \mathrm{e}^{\eta L} + \mathrm{e}^{-\eta L} - 2\right]}{(1-\gamma)\,\mathrm{e}^{\eta L} - (1+\gamma)\,\mathrm{e}^{-\eta L}}\,, \tag{B.4}$$

where $\gamma = (1+\theta)L\eta/\theta$.

The solution is greatly simplified if water and solid grains compressibilities are neglected, so that $\gamma = 0$, which yields

$$\widehat{p}(x,s) = \frac{q_0}{k/\mu}\,\frac{1}{s\,\eta}\,\frac{\mathrm{e}^{-\eta x} - \mathrm{e}^{-\eta(L-x)} - \mathrm{e}^{-\eta L} + 1}{\mathrm{e}^{-\eta L} + 1}\,. \tag{B.5}$$

Laplace inversion of this equation yields the solution in space and time domains (Eq. (20)).

If the hydraulic condition at $x = L$ is of no flow, then Eq. (B.3a) still holds at $x = 0$, but the BC at the outer boundary becomes

$$\left.\frac{\partial \widehat{p^*}(x,s)}{\partial x}\right|_{x=L} = 0 \tag{B.6}$$

and the solution for $p^*(x,t)$ is

$$\widehat{p^*}(x,s) = \frac{q_0}{k/\mu}\,\frac{1}{s\,\eta}\,\frac{\mathrm{e}^{-\eta x} + \mathrm{e}^{-\eta(2L-x)}}{1 - \mathrm{e}^{-2\eta L}}\,, \tag{B.7}$$

which can be inverted. After adding the spatial average of pressure $\overline{p}$ (Eq. (24)), the solution is given by Eq. (25).

C: Volumetric deformation in cylindrical domain

In the case of radial axisymmetry, the equilibrium equation in radial direction results

$$\frac{\partial \sigma_r}{\partial r} + \frac{\sigma_r - \sigma_\theta}{r} = 0\,, \tag{C.1}$$

where we have considered that $\tau_{rz} = 0$, which is valid for both plane stress and plane strain conditions.

Plane strain

Application of Hooke's law [*Jaeger et al.*, 2007] for the case of plane strain in direction z ($\varepsilon_z = 0$) yields

$$\frac{\partial^2 u_r}{\partial r^2} + \frac{1}{r}\frac{\partial u_r}{\partial r} - \frac{1}{r^2}u_r = \frac{b}{2G+\lambda}\,\frac{\partial p}{\partial r}\,, \tag{C.2}$$

where $b/(2G+\lambda)$ can be substituted with α_{p1}. This equation can be integrated to yield [*De Simone et al.*, 2017]

$$u_r = \alpha_{p1}\left[\frac{1}{r}\int_{r0}^{r} r\,p(r,t)dr + Cr + \frac{D}{r}\right] \tag{C.3}$$

and the volumetric deformation is

$$\varepsilon_{vol} = \frac{\partial u_r}{\partial r} + \frac{u_r}{r} = \alpha_{p1}\Big[p(r,t) + 2C\Big]\,, \tag{C.4}$$

where constants C and D depend on the mechanical BC at the surfaces $r = r_0$ and $r = R$. We consider zero radial displacements or imposed stress boundary conditions for the inner and outer boundary conditions, which defines the four scenarios presented in Table C.1 together with the respective values of the constant C. In the case in which r_0 is small such that its squared value can be disregarded, the values of C are not dependent on the inner BC, but are mostly dependent on the outer BC.

Table C.1. Values of the constant C in equation C.3. Approximated values refer to the case in which r_0 is small such that its squared value can be disregarded. Notice that in this condition, the value of C is not dependent on the inner boundary condition.

BCs	**Constant C for plane strain**
$u_r(r_0) = 0$ $u_r(R) = 0$	$-\dfrac{1}{R^2 - r_0^2}\displaystyle\int_{r_0}^{R} r\, p(r,t)dr \;= -\dfrac{\overline{p}(t)}{2}$
$u_r(r_0) = 0$ $\sigma_r(R) = 0$	$\dfrac{2G}{(2G+2\lambda)R^2 + 2Gr_0^2}\displaystyle\int_{r_0}^{R} rp(r,t)dr \approx \dfrac{G}{G+\lambda}\dfrac{\overline{p}(t)}{2} = (1-2\nu)\dfrac{\overline{p}(t)}{2}$
$\sigma_r(r_0) = -p(r_0)$ $u_r(R) = 0$	$-\dfrac{1}{(2G+2\lambda)r_0^2 + 2GR^2}\left[(2G+\lambda)r_0^2 p(r_0,t) + 2G\displaystyle\int_{r_0}^{R} rp(r,t)dr\right] \approx -\dfrac{\overline{p(t)}}{2}$
$\sigma_r(r_0) = -p(r_0)$ $\sigma_r(R) = 0$	$\dfrac{(1-\nu)r_0^2}{R^2 - r_0^2}p(r_0,t) + \dfrac{(1-2\nu)}{R^2 - r_0^2}\displaystyle\int_{r_0}^{R} r\, p(r,t)dr \approx (1-2\nu)\dfrac{\overline{p}(t)}{2}$

Plane stress

If plane stress in direction z ($\sigma_z = 0$) is considered, it results

$$\varepsilon_z = \frac{bp}{2G+\lambda} - \frac{\lambda}{2G+\lambda}(\varepsilon_r + \varepsilon_\theta)\,. \tag{C.5}$$

Therefore, the equilibrium equation ends up into

$$\frac{\partial^2 u_r}{\partial r^2} + \frac{1}{r}\frac{\partial u_r}{\partial r} - \frac{1}{r^2}u_r = \frac{b}{2(G+\lambda)}\frac{\partial p}{\partial r}\,, \tag{C.6}$$

593 which returns

$$u_r = \frac{b}{2(G+\lambda)}\left[\frac{1}{r}\int_{r0}^{r} r\, p(r,t)dr + Cr + \frac{D}{r}\right] . \tag{C.7}$$

594 The volumetric deformation is, thus, given by

$$\varepsilon_{vol} = \frac{\partial u_r}{\partial r} + \frac{u_r}{r} + \varepsilon_z = \alpha_{p2}\left(p(r,t) + \frac{1-2\nu}{1-\nu}C\right) , \tag{C.8}$$

595 where $b/(G+\lambda)$ have been substituted by α_{p2}. The values of the constant C for every
596 scenario of mechanical BCs is reported in Table C.2.

597 **Table C.2.** Values of the constant C in equation C.7. Approximated values refer to the case in which r_0
598 is small such that its squared value can be disregarded. Notice that in this condition, the value of C is not
599 dependent on the inner boundary condition.

BCs	**Constant C for plane stress**
$u_r(r_0) = 0$ $u_r(R) = 0$	$-\frac{1}{R^2 - r_0^2}\int_{r_0}^{R} r\, p(r,t)dr = -\frac{\overline{p}(t)}{2}$
$u_r(r_0) = 0$ $\sigma_r(R) = 0$	$\frac{2G+\lambda}{(2G+3\lambda)R^2 + (2G+\lambda)r_0^2}\int_{r_0}^{R} r p(r,t)dr \approx \frac{2G+\lambda}{2G+3\lambda}\frac{\overline{p}(t)}{2} = \frac{1-\nu}{1+\nu}\frac{\overline{p}(t)}{2}$
$\sigma_r(r_0) = -p(r_0)$ $u_r(R) = 0$	$-\frac{2G+\lambda}{(2G+3\lambda)r_0^2 + (2G+\lambda)R^2}\left[\frac{r_0^2}{1-2\nu}p(r_0,t) + \int_{r_0}^{R} r\, p(r,t)dr\right] \approx -\frac{\overline{p}(t)}{2}$
$\sigma_r(r_0) = -p(r_0)$ $\sigma_r(R) = 0$	$\frac{2G+\lambda}{(2G+3\lambda)(r_0^2 + R^2)}\left[\frac{r_0^2}{1-2\nu}p(r_0,t) + \int_{r_0}^{R} r\, p(r,t)dr\right] \approx \frac{1-\nu}{1+\nu}\frac{\overline{p}(t)}{2}$

600 D: HM Pressure solution for cylindrical domain

601 Laplace transform with respect to time of Eq. (32) yields

$$\frac{\partial^2 \widehat{p^*}(r,s)}{\partial r^2} + \frac{1}{r}\frac{\partial \widehat{p^*}(r,s)}{\partial r} - \frac{s}{D}\,\widehat{p^*}(r,s) , \tag{D.1}$$

602 where s is the Laplace variable and the hat denotes the functions in Laplace space. Its
603 general solution is of the type [*Carslaw and Jaeger*, 1959]

$$\widehat{p^*}(r,s) = C_1\, I_0(\eta r) - \frac{2}{\pi}\, C_2\, K_0(\eta r) , \tag{D.2}$$

604 where $\eta = \sqrt{s/D}$, whereas I_0 and K_0 represent the modified Bessel functions of first and
605 second kind, respectively, of order zero. Constants C_1 and C_2 are obtained by applying the

hydraulic boundary conditions. As in the linear flow case, we assume constant injection Q_0 at the inner boundary ($r = r_0$), and either constant pressure or zero flow at the outer boundary ($r = R$).

In the first case, the boundary conditions in the Laplace domain are

$$\begin{cases} \lim_{r\to 0}\left(r\,\dfrac{\partial \widehat{p^*}(r,s)}{\partial r}\right) = -\dfrac{Q_0}{2\pi k/\mu}\,\dfrac{1}{s} & \text{(D.3a)} \\ \displaystyle\int_{r_0}^{R} r\,\widehat{p^*}(r,s)dr = \dfrac{1+\theta}{\theta}\,\dfrac{R^2-r_0^2}{2}\,\widehat{p^*}(R,s)\,. & \text{(D.3b)} \end{cases}$$

After calculation of derivatives and integrals of the Bessel functions [*Abramowitz and Stegun*, 1964], the constants are obtained:

$$C_1 = \frac{2}{\pi}\,\frac{Q_0}{4k/\mu}\,\frac{1}{s}\left[\frac{RK_1(R\eta) - r_0K_1(r_0\eta) + \gamma K_0(R\eta)}{RI_1(R\eta) - r_0I_1(r_0\eta) - \gamma I_0(R\eta)}\right], \tag{D.4}$$

$$C_2 = -\frac{Q_0}{4k/\mu}\,\frac{1}{s}\,, \tag{D.5}$$

where

$$\gamma = \frac{1+\theta}{\theta}\,\frac{R^2-r_0^2}{2}\,\eta \tag{D.6}$$

and I_1 and K_1 represent the modified Bessel functions of first and second kind, respectively, of the first order. Notice that $C1$ and $C2$ depend also on the mechanical BCs and on the condition of plane stress or plane strain in the z direction because they depend on θ (Eq. 31c).

Once $\widehat{p^*}(r,s)$ is defined, Eq. (35) allows to yield the solution for the pressure in the Laplace domain (Eq. (36)).

In the second case, that is, in the case the flow rate is zero at the outer boundary, Eq. (D.3a) still holds at $r = r_0$, but the BC at $r = R$ becomes

$$\left.\frac{\partial \widehat{p^*}(r,s)}{\partial r}\right|_{r=R} = 0\,. \tag{D.7}$$

Hence, the constants can be easily derived:

$$C_1 = \frac{2}{\pi}\,\frac{Q_0}{4k/\mu}\,\frac{1}{s}\,\frac{K_1(R\eta)}{I_1(R\eta)}\,, \tag{D.8}$$

$$C_2 = -\frac{Q_0}{4k/\mu}\,\frac{1}{s}\,. \tag{D.9}$$

In order to obtain the solution for pressure, we need to add the average value of pressure to $\widehat{p^*}(r,s)$, which we define in the real space in Eq. (40). We transform it into Laplace domain, in order to give the complete expression for the pressure in the Laplace domain (Eq. (43)).

Acknowledgments

The authors are grateful to Dr. Paul Hsieh (USGS) for valuable reviews that improved this manuscript. We also acknowledge Larry Murdoch, Thomas J. Burbey and an anonymous reviewer for the kind assessments. Discussions with A. Comolli have been significantly appreciated. We thank B.M. Gómez-Castro who performed some of the numerical simulations used to test the analytical solutions. Financial support from the "TRUST" project (European Community's Seventh Framework Programme FP7/2007-2013 under grant agreement n 309607) and from "FracRisk" project (European Community's Horizon 2020 Framework Programme H2020-EU.3.3.2.3 under grant agreement n 640979) is acknowledged. Data presented in the figures can be obtained by applying the analytical solutions presented in the manuscript. We also provide these data as Supplementary Information.

References

Abramowitz, M., and I. A. Stegun (1964), Handbook of mathematical functions: with formulas, graphs, and mathematical tables, *Courier Corporation*, *55*.

Batchelor, A.S. (1983), Hot dry rock reservoir stimulation in the UK an extended summary, *International seminar on the results of EC geothermal energy research*, *3*, 681-711.

Bear, J., and M. Y. Corapcioglu (1981), Mathematical model for regional land subsidence due to pumping: 2. Integrated aquifer subsidence equations for vertical and horizontal displacements, *Water Resources Research*, *17*(4), 947–958, doi: 10.1029/WR017i004p00947.

Berg, S. J., P. a. Hsieh, and W. a. Illman (2011), Estimating hydraulic parameters when poroelastic effects are significant., *Groundwater*, *49*(6), 815–29, doi:10.1111/j.1745-6584.2010.00781.x.

Biot, M. A. (1941), General theory of three-dimensional consolidation, *Journal of Applied Physics*, *12*(2), 155–164.

Blöcher, G., Moeck, I., Milsch, H. and Zimmermann, G. (2008), Modelling of pore pressure response due to hydraulic stimulation treatments at the geothermal research dou-

649 blet EGRSK3/90 and GTGRSK4/05 in summer 2007., *Proc. Thirty-Third Workshop on*
650 *Geothermal Reservoir Engineering, Stanford University, Stanford, California, January*
651 *28-30, 2008*, *4026* (4086), 60.

652 Burbey, T. J. (1999), Effects of horizontal strain in estimating specific storage and com-
653 paction in confined and leaky aquifer systems, *Hydrogeology Journal*, *7*(6), 521–532,
654 doi:10.1007/s100400050225.

655 Burbey, T. J. (2001), Storage coefficient revisited: Is purely vertical strain a good assump-
656 tion?, *Ground Water*, *39*(3), 458–464.

657 Carslaw, H. S., and J. C. Jaeger (1959), Conduction of heat in solids, *Oxford: Clarendon*
658 *Press, 1959, 2nd ed.*

659 Chen, C.-S. (1984), A reinvestigation of the analytical solution for drawdown distributions
660 in a finite confined aquifer, *Water Resources Research*, *20*(10), 1466–1468.

661 CIMNE, Kratos (2012) - www.cimne.com/kratos/.

662 Coussy, O. (2004), Poromechanics, *John Wiley & Sons,2004*.

663 Dadvand P., R. Rossi, and E. Oñate (2010), An object-oriented environment for develop-
664 ing finite element codes for multi-disciplinary applications, *Arch Comput Methods Eng*
665 *17(3)*, 253–297.

666 de Marsily, G. (1981), Quantitative hydrogeology., *Academic Press*.

667 De Simone, S., J. Carrera, and B. M. Gómez-Castro (2017), A practical solution to the
668 mechanical perturbations induced by non-isothermal injection into a permeable medium,
669 *International Journal of Rock Mechanics and Mining Sciences*, *91*, 7–17.

670 Detournay, E., and A. A. H.-D. Cheng (1993), Fundamentals of poroelasticity, *Chapter*
671 *5 in Comprehensive Rock Engineering: Principles, Practice and Projects, II*, *II*, doi:
672 10.1016/0148-9062(94)90606-8.

673 Gambolati, G. (1974), Second-order theory of flow in three-dimensional deforming media,
674 *Water Resources Research*, *10*(6), 1217–1228, doi:10.1029/WR010i006p01217.

675 Gómez-Castro, B. M., S. De Simone, R. Rossi, A. Larese De Tetto, and J. Carrera (2015),
676 Development of a finite element code to solve thermo-hydro-mechanical coupling and
677 simulate induced seismicity., *EGU General Assembly Conference Abstracts*, *17*.

678 Hantush, M. S. (1961), Drawdown around a partially penetrating well, *Journal of the Hy-*
679 *draulics Division*, *87*(4), 83–98.

680 Helm, D. C. (1994), Horizontal aquifer movement in a Theis-Thiem confined system, *Wa-*
681 *ter Resources Research*, *30*(4), 953–964, doi:10.1029/94WR00030.

Hsieh, P. A. (1996), Deformation-induced changes in hydraulic head during ground-water withdrawal, *Ground Water*, *34*(6), 1082–1089, doi:10.1111/j.1745-6584.1996.tb02174.x.

Hsieh, P. a., and R. L. Cooley (1995), Comment on âĂIJHorizontal aquifer movement in a Theis-Thiem Confined SystemâĂİ by Donald C. Helm, *Water Resources Research*, *31*(12), 3107–3111, doi:10.1029/95WR02713.

Jacob, C. E. (1940), On the flow of water in an elastic artesian aquifer, *Eos, Transactions American Geophysical Union*, *21*(2), 574–586.

Jaeger, J. C., N. G. Cook, and R. Zimmerman (2007), Fundamentals of rock mechanics., *Blackwell Publishing*.

Langguth, H., and C. Treskatis (1989), Reverse water level fluctuations in semiconfined aquifer systemsâĂŤâĂIJRhade effectâĂİ, *Journal of Hydrology*, *109*(1), 79–93.

Meier, P. M., J. Carrera, and X. Sánchez-Vila (1998), An evaluation of Jacob's method for the interpretation of pumping tests in heterogeneous formations, *Water Resources Research*, *34*(5), 1011–1025.

Meinzer, O. E. (1928), Compressibility and elasticity of artesian aquifers, *Economic Geology*, *23*(3), 263–291.

Mitchell, J. K., K. Soga, et al. (2005), Fundamentals of soil behavior, *John Wiley & Sons Hoboken, NJ*.

Murdoch, L. C., and L. N. Germanovich (2012), Storage change in a flat-lying fracture during well tests, *Water Resources Research*, *48*(12).

Narasimhan, T. (2006), On Storage Coefficient and Vertical Strain, *Ground Water*, *44*(3), 488–491, doi:10.1111/j.1745-6584.2006.00160.x.

Narasimhan, T., and B. Kanehiro (1980), A note on the meaning of storage coefficient, *Water Resources Research*, *16*(2), 423–429.

Nur, A., and J. Byerlee (1971), An exact Effective Stress Law for Elastic Deformation of Rock with Fluids, *Journal of Geophysical Research*, *76*(26), 6414–6419.

Olivella, S., Carrera, J., Gens, A., and Alonso, E. E. (1994), Nonisothermal multiphase flow of brine and gas through saline media. *Transport in porous media, 15(3), 271-293*.

Olivella, S., A. Gens, J. Carrera, and E. Alonso (1996), Numerical formulation for a simulator (CODE_BRIGHT) for the coupled analysis of saline media. *Eng Comput. 13(7):87âĂŞ112*.

Poland, J. F., and G. H. Davis (1969), Land subsidence due to withdrawal of fluids, *Reviews in engineering geology*, *2*, 187–270.

Pujades, E., S. De Simone, J. Carrera, E. Vázquez-Suñé, and A. Jurado (2017), Settlements around pumping wells: analysis of influential factors and a simple calculation procedure., *Journal of Hydrology, 548, 225-236*.

Renard, P., and G. De Marsily (1997), Calculating equivalent permeability: a review, *Advances in water resources*, *20*(5), 253–278.

Rice, J., and M. Cleary (1976), Some basic stress diffusion solutions for fluid-saturated elastic porous media with compressible constituents, *Reviews of Geophysics*, *14*(2).

Sanchez-Vila, X., P. M. Meier, and J. Carrera (1999), Pumping tests in heterogeneous aquifers: An analytical study of what can be obtained from their interpretation using Jacob's method, *Water Resources Research*, *35*(4), 943–952.

Sanchez-Vila, X., A. Guadagnini, and J. Carrera (2006), Representative hydraulic conductivities in saturated groundwater flow, *Reviews of Geophysics*, *44*(3).

Slack, T., Z. Murdoch, L. C. and Germanovich, L. N. and Hisz, D. B. (2013), Reverse water-level change during interference slug tests in fractured rock, *Water Resources Research*, *49*, 1552-1567.

Terzaghi, K. (1923), Die Berechnung der DurchlÃđssigkeitziffer des Tones aus dem Verlauf der hydrodynamischen Spannungs- erscheinungen, *Akad Wissensch Wien Sitzungsber Math- naturwissensch Klasse IIa*, *142(3/4)*.

Verruijt, A. (1969), Elastic Storage of Aquifers, in: Flow through Porous Media (R.J.M. De Wiest, editor), *Academic Press, New York*.

Verruijt, A. (2013), Theory and problems of poroelasticity, *Delft University of Technology*.

Wang, H. F. (2000), Theory of linear poroelasicity with applications to geomechanics and hydrogeology, *Princeton University Press*.

Yin, S., M. B. Dusseault, and L. Rothenburg (2007), Coupled multiphase poroelastic analysis of reservoir depletion including surrounding strata, *International Journal of Rock Mechanics and Mining Sciences*, *44*(5), 758–766, doi:10.1016/j.ijrmms.2006.11.005.

Zimmerman, R. (2000), Coupling in poroelasticity and thermoelasticity, *International Journal of Rock Mechanics and Mining Sciences*, *37*(1-2), 79–87, doi:10.1016/S1365-1609(99)00094-5.